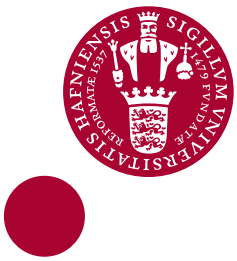

# lncRNA Panct1 Maintains Mouse Embryonic Stem Cell Identity by Regulating TOBF1 Recruitment to Oct-Sox Sequences in Early G1

Chakraborty, Debojyoti; Paszkowski-Rogacz, Maciej; Berger, Nicolas; Ding, Li; Mircetic, Jovan; Fu, Jun; Iesmantavicius, Vytautas; Choudhary, Chunaram; Anastassiadis, Konstantinos; Stewart, A Francis; Buchholz, Frank

*Published in:*
Cell Reports

*DOI:*
10.1016/j.celrep.2017.11.045

*Publication date:*
2017

*Document version*
Publisher's PDF, also known as Version of record

Cell Reports

Report

# lncRNA *Panct1* Maintains Mouse Embryonic Stem Cell Identity by Regulating TOBF1 Recruitment to Oct-Sox Sequences in Early G1

## Graphical Abstract

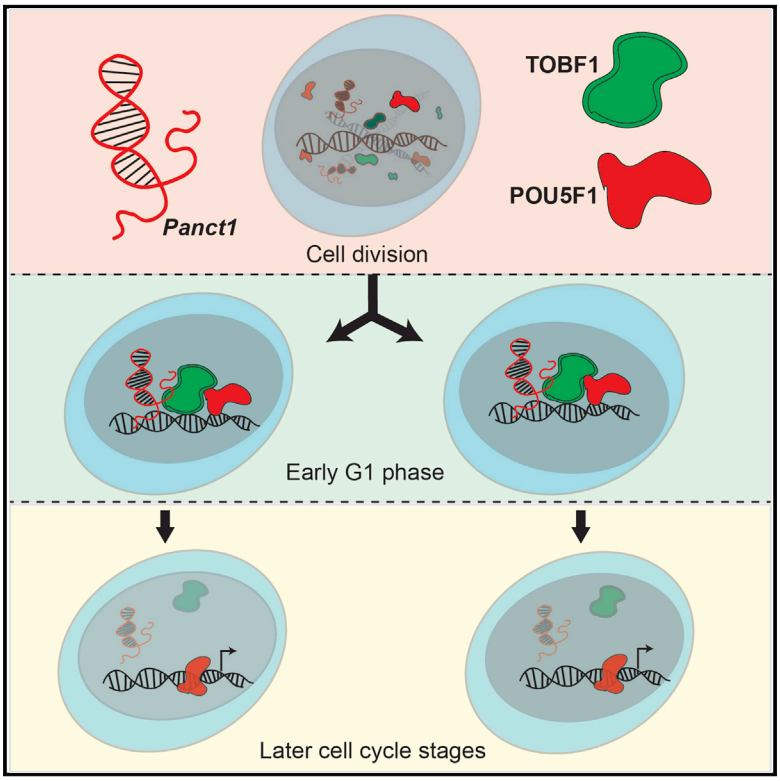


## Highlights

- lncRNA *Panct1* regulates the transient recruitment of TOBF1 to Oct-Sox motifs
- *Panct1* physically interacts with TOBF1 in a cell-cycle-specific manner
- *Panct1* might function as a barcode for identifying genomic addresses

## Authors

Debojyoti Chakraborty, Maciej Paszkowski-Rogacz, Nicolas Berger, ..., Konstantinos Anastassiadis, A. Francis Stewart, Frank Buchholz

## Correspondence

frank.buchholz@tu-dresden.de

## In Brief

Chakraborty et al. molecularly characterize the lncRNA *Panct1* in the maintenance of ESC identity. Their study reveals the tightly controlled, cell-cycle-dependent modulation of gene expression cooperatively mediated by *Panct1* and the DNA-interacting protein TOBF1. Hence, lncRNAs might serve as barcodes for identifying genomic addresses that regulate cellular states.

## Data and Software Availability

GSE73806

Chakraborty et al., 2017, Cell Reports *21*, 3012–3021
December 12, 2017 
https://doi.org/10.1016/j.celrep.2017.11.045

CellPress

OPEN ACCESS
CellPress

Cell Reports
Report

# lncRNA *Panct1* Maintains Mouse Embryonic Stem Cell Identity by Regulating TOBF1 Recruitment to Oct-Sox Sequences in Early G1

Debojyoti Chakraborty,[1,8] Maciej Paszkowski-Rogacz,[1] Nicolas Berger,[1] Li Ding,[1] Jovan Mircetic,[1] Jun Fu,[2] Vytautas Iesmantavicius,[3] Chunaram Choudhary,[3] Konstantinos Anastassiadis,[4] A. Francis Stewart,[2] and Frank Buchholz[1,5,6,7,9,*]

[1]Medical Systems Biology, UCC, Medical Faculty Carl Gustav Carus, TU Dresden, Fetscherstrasse 74, 01307 Dresden, Germany
[2]Genomics, Biotechnology Center, TU Dresden, BioInnovationsZentrum, Tatzberg 47, 01307 Dresden, Germany
[3]The Novo Nordisk Foundation Center for Protein Research, University of Copenhagen, Copenhagen, Denmark
[4]Stem Cell Engineering, Biotechnology Center, TU Dresden, BioInnovationsZentrum, Tatzberg 47, 01307 Dresden, Germany
[5]Max Planck Institute of Molecular Cell Biology and Genetics, 01307 Dresden, Germany
[6]German Cancer Research Center (DKFZ), Heidelberg and German Cancer Consortium (DKTK) partner site Dresden, 01307 Dresden, Germany
[7]National Center for Tumor Diseases (NCT), University Hospital Carl Gustav Carus, TU Dresden, 01307 Dresden, Germany
[8]Present address: CSIR, Institute of Genomics and Integrative Biology, Mathura Road, New Delhi 110025, India
[9]Lead Contact
*Correspondence: frank.buchholz@tu-dresden.de
https://doi.org/10.1016/j.celrep.2017.11.045

## SUMMARY

**Long noncoding RNAs (lncRNAs) have been implicated in diverse biological processes, including embryonic stem cell (ESC) maintenance. However, their functional mechanisms remain largely undefined. Here, we show that the lncRNA *Panct1* regulates the transient recruitment of a putative X-chromosome-encoded protein A830080D01Rik, hereafter referred to as transient octamer binding factor 1 (TOBF1), to genomic sites resembling the canonical Oct-Sox motif. TOBF1 physically interacts with *Panct1* and exhibits a cell-cycle-specific punctate localization in ESCs. At the chromatin level, this correlates with its recruitment to promoters of pluripotency genes. Strikingly, mutating an octamer-like motif in *Panct1* RNA abrogates the strength of TOBF1 localization and recruitment to its targets. Taken together, our data reveal a tightly controlled spatial and temporal pattern of lncRNA-mediated gene regulation in a cell-cycle-dependent manner and suggest that lncRNAs might function as barcodes for identifying genomic addresses for maintaining cellular states.**

## INTRODUCTION

Long noncoding RNAs (lncRNAs) are known to play diverse functional roles in a multitude of different biological pathways including disease progression, developmental regulation, and maintenance of cellular states (Engreitz et al., 2016). lncRNA-mediated regulation is a vital component of a cell's intrinsic ability to divide, proliferate, and differentiate, with lncRNA perturbations frequently giving rise to phenotypic alterations to normal cellular behavior (Ulitsky and Bartel, 2013). This is particularly true in the case of embryonic stem cells (ESCs), where subtle changes in lncRNA expression can lead to a loss of self-renewal and differentiation (Martello and Smith, 2014; Young, 2011). In recent years, a number of lncRNAs have been classified as being involved in the determination of ESC fate in both mouse and human (Dinger et al., 2008; Sheik Mohamed et al., 2010; Loewer et al., 2010; Guttman et al., 2011; Chakraborty et al., 2012; Lin et al., 2014), often by altering the local chromatin architecture to generate important cues for pluripotency (Tsai et al., 2010; Guttman et al., 2011; Hacisuleyman et al., 2014; McHugh et al., 2015). However, the spatial and temporal aspects governing such events have not been explored in detail.

We previously identified an X-chromosome-associated intronic lncRNA termed *Panct1* from an RNAi screen that affected *Pou5f1* (also known as *Oct4*) expression (Chakraborty et al., 2012). Here, we present its molecular characterization and show that *Panct1* regulates and interacts with the previously uncharacterized protein A830080D01Rik, hereafter referred to as transient octamer binding factor 1 (TOBF1), to influence mouse ESC fate.

## RESULTS

### *Panct1* Is a Sense Intronic lncRNA Localizing in the Nucleus

*Panct1* is encoded from the X chromosome in sense orientation from the first intron of the putative protein-coding gene *Tobf1* (Figure 1A). To better characterize *Panct1*, we performed northern blot, 5′ RACE, 5′ cap, and RNA fluorescence *in situ* hybridization (FISH) assays and classified *Panct1* as a ~3.6 kb, capped, and polyadenylated transcriptional unit that predominantly localizes to the nucleus (Figures 1B–1D and S1A). RNAi and

 

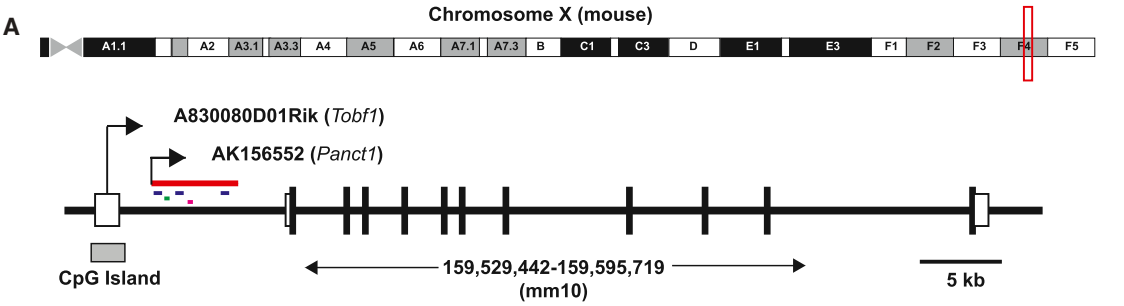


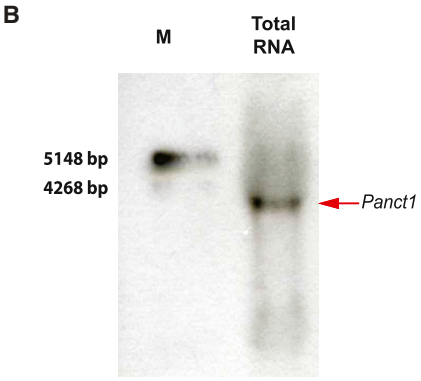


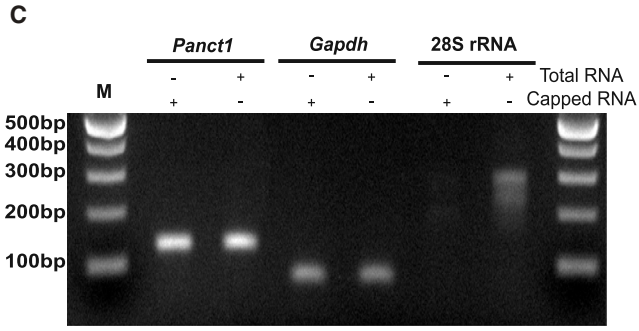


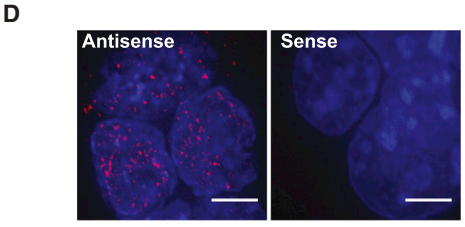


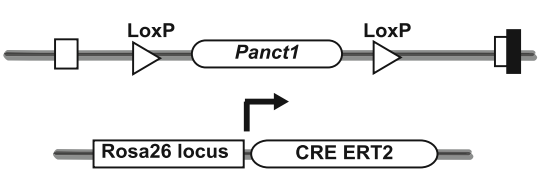


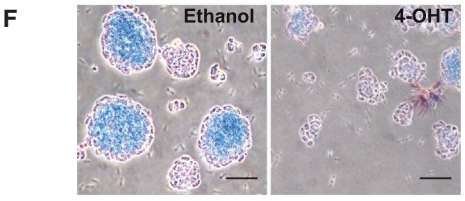


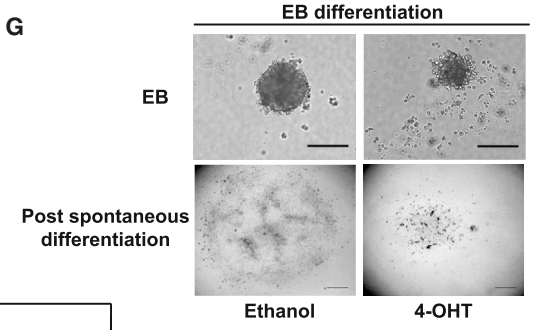


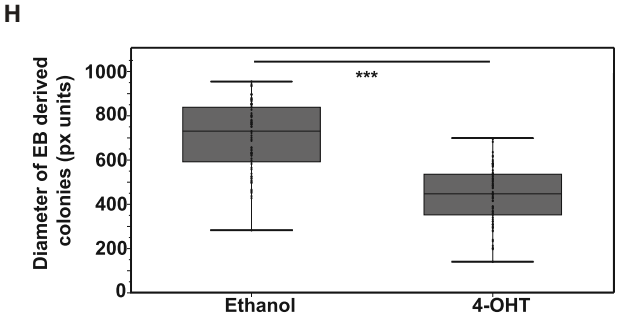


*(legend on next page)*

overexpression of *Tobf1* did not lead to concomitant changes in the levels of *Panct1*, establishing that *Panct1* and *Tobf1* are independent transcripts (Figures S1B and S1C).

### *Panct1* Knockout Affects ESC Survival and Pluripotency

To extend the functional analysis of *Panct1*, we generated a conditional knockout (KO) allele of *Panct1* in ESCs in which the *Panct1* gene can be deleted upon administration of 4-hydroxy tamoxifen (4-OHT) (Figure 1E). Complete excision of *Panct1* was confirmed using Southern hybridization and PCR 48 hr after administration of 4-OHT, which led to activation of Cre and subsequent *Panct1* deletion in these cells (Figures S1D–S1F). Using both 4-OHT-mediated and plasmid-based Cre expression, we observed that *Panct1* KO cells recapitulated the observed phenotype upon *Panct1* RNAi (Chakraborty et al., 2012), including profound morphological changes to ESCs characterized by smaller colony size and loss of alkaline phosphatase (AP) staining (Figures 1F and S1G–S1I); a reduction in the level of pluripotency markers *Pou5f1*, *Nanog*, *Sox2*, *Rex1*, and *Klf4* (Figure S1J); upregulation of lineage markers *Fgf5* and *Gata4* (Figure S1K); and reduced viability (Figure S1L). Defects in pluripotency-related genes often lead to alterations of developmental programs (Aksoy et al., 2014). To monitor if *Panct1* deletion affects differentiation of ESCs, we monitored the formation of embryoid bodies (EB) from *Panct1* KO ESCs and observed that *Panct1*-negative EBs failed to grow upon spontaneous differentiation, suggesting that *Panct1* deficiency compromises ESC differentiation *in vitro* (Figures 1G and 1H).

### *Panct1* Overexpression Supports Maintenance of Pluripotency

Next, we sought to determine if the KO phenotype could be rescued by exogenous expression of *Panct1*. Notably, re-expressing *Panct1* rescued the colony size and AP staining phenotype and led to a higher expression of pluripotency genes *Pou5f1*, *Nanog*, *Zscan4c*, *Sox2*, and *Klf4* without significant changes to the expression of *Fgf5* and *Gata4* (Figures S2A–S2E). Thus, exogenous expression of *Panct1* can rescue its KO phenotype.

To determine whether exogenous *Panct1* expression can influence *in vitro* differentiation of mouse ESCs, we grew *Panct1*-overexpressing cells in the absence of leukemia inhibitory factor (−LIF) and compared them to controls. We observed four times higher levels in AP staining accompanied by an increase in mRNA levels of pluripotency markers *Pou5f1*, *Nanog*, and *Zscan4c* in *Panct1*-overexpressing cells, suggesting that under differentiating conditions, overexpression of *Panct1* facilitates retention of the pluripotent character of ESCs (Figures S2F–S2H).

### *Panct1* Physically Interacts with TOBF1 Protein and Regulates Its Subcellular Localization

Recent reports have demonstrated cross-talk between lncRNAs and their neighboring genes, particularly in cases of intronic lncRNAs (Heo and Sung, 2011; Guil et al., 2012; Li et al., 2015). Interestingly, upon endoribonuclease prepared small interfering RNA (esiRNA)-mediated depletion of *Tobf1*, a concomitant reduction of the key pluripotency markers *Pou5f1* and *Klf4* was seen (Figure 2A), while ESCs undergoing differentiation showed a gradual loss of *Tobf1* levels (Figure 2B). Additionally, knockdown of *Tobf1* caused morphological changes of ESC colonies and loss of AP staining (Figures 2C and 2D). Taken together, these results indicated that *Tobf1* is required to maintain the pluripotent ESC state.

Since the *Tobf1* phenotype phenocopied *Panct1*, we next inquired if they both act in the same pathway either by transcriptionally regulating each other's expression or by lncRNA:protein association. Since *Panct1* KO cells did not show a drastic reduction in *Tobf1* levels and *Tobf1* perturbation did not affect *Panct1* levels (Figures S3A, S1B, and S1C), we examined if they interact physically.

To study TOBF1 protein, we generated stable TOBF1-GFP-expressing mouse ESC lines by bacterial artificial chromosome (BAC) transgenomics, allowing visualization and purification of the protein under near-physiological expression conditions (Poser et al., 2008; Kittler et al., 2005; Hutchins et al., 2010) (Figure 2E). Interestingly, BAC-tagged TOBF1 showed a gradual loss of expression in ESCs undergoing differentiation, confirming its downregulation upon exit from pluripotency (Figure 2F).

We then proceeded to determine the subcellular localization of TOBF1 and observed that the majority of ESCs showed a diffuse TOBF1 localization in the nucleus with a few cells appearing to

**Figure 1. Characterization of *Panct1***

(A) Genomic visualization of the A830080D01Rik (*Tobf1*) gene showing the intronic position of *Panct1* (red). Black squares depict exons, and white squares show the UTRs of the putative protein-coding gene. Blue, green, and pink bars represent the position of probes for northern blot and primers for 5′ RACE and exonuclease assay, respectively. The chromosome coordinates from the genome assembly version mm10 are presented.

(B) Northern blot showing expression of *Panct1* as a ~3.6-kb transcript (arrow). DIG-labeled DNA molecular weight marker (M) is shown on the left lane.

(C) Terminator 5′ exonuclease assay showing presence of a 5′ cap on *Panct1.* Gapdh and 28S rRNA served as positive and negative controls, respectively.

(D) Representative images of RNA FISH showing cellular localization of *Panct1* in mouse ESCs. Samples hybridized with an antisense probe (left) and a sense control (right) are shown (red, FISH signal; blue, DAPI; scale bars, 5 μm).

(E) Schematic of the *Panct1* knockout allele. White triangles denote positions of the *loxP* sites. White and black rectangles represent the position of exons in *Tobf1*.

(F) Representative image of AP staining of *Panct1* knockout cells 5 days after administration of 4-OHT as compared to ethanol-treated control cells. Scale bars, 50 μm.

(G) Representative image of embryoid bodies (in top panel) and colonies formed after spontaneous differentiation into the germ layers derived from control or *Panct1* knockout cells. Scale bars represent 50 μm (top) and 100 μm (bottom). Note defects in growth upon spontaneous differentiation in *Panct1* knockout EBs.

(H) Boxplots depicting diameter of EB-derived colonies (in pixel units) from ethanol-treated (n = 80 EBs) or 4-OHT-treated (n = 77 EBs) cells. Whiskers denote positive or negative deviations from the mean. ***$p < 0.005$ (two-tailed Student's t test).

See also Figures S1 and S2.

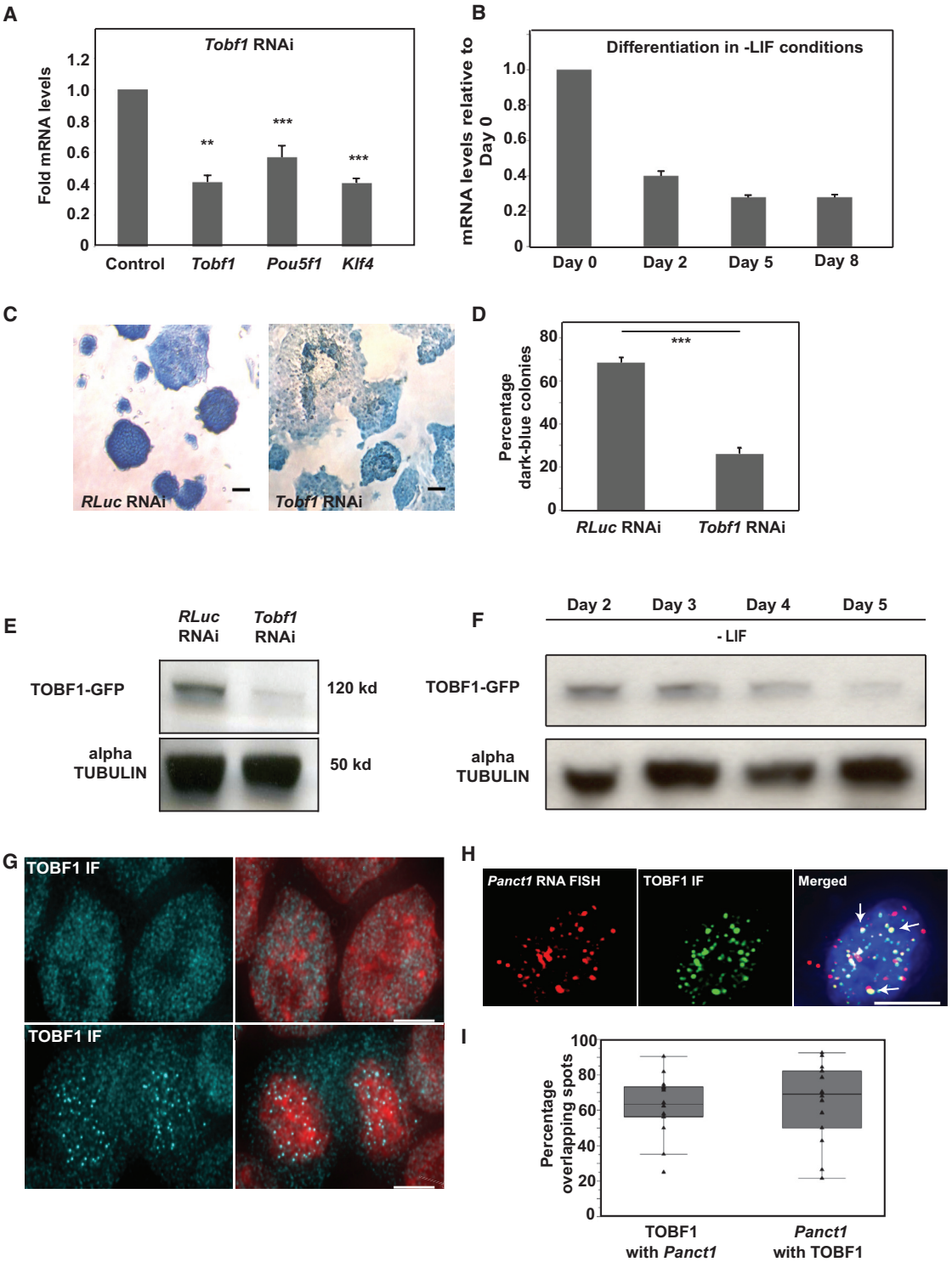


**Figure 2. Tobf1 Is a Determinant of Mouse ESC Fate**

(A) qRT-PCR showing depletion of pluripotency markers *Pou5f1* and *Klf4* upon *Tobf1* knockdown in ESCs. Error bars indicate the SEM from three biological replicates.

(B) *Tobf1* mRNA levels at indicated time points (in ESCs undergoing differentiation by removal of LIF) relative to levels at day 0. Error bars indicate the SEM from three replicates.

(C) AP staining in cells with *Tobf1* RNAi and control (Renilla Luciferase). RNAi shows exit from pluripotency marked by loss of AP and flattened colony morphology upon *Tobf1* depletion. Staining performed 72 hr post-RNAi.

*(legend continued on next page)*

have bright punctate foci (Figure 2G). Intriguingly, *Panct1* RNA FISH performed together with TOBF1-GFP immunostaining showed ~70% overlap between the *Panct1* and the TOBF1 foci signals, suggesting that lncRNA and the protein colocalize in these cells (Figures 2H and 2I). To inquire what led to the formation of these foci, we transfected a histone-2B-expressing plasmid into the TOBF1 BAC-tagged cell line and used time-lapse microscopy to dissect cell division events. Every cell showed the formation of the bright TOBF1 foci immediately following mitosis in the early G1 phase (Figure 3A; Movie S1). The two newly formed daughter nuclei displayed on average 68 bright spots that persisted for approximately 30 min before disappearing (Figures 3A and S3B). To study TOBF1 in relation to other nuclear foci-forming factors, we performed TOBF1 co-immunofluorescence (coIF) with several foci-forming structures in cells such as telomeres, centromeres, or CDK9 but did not observe a significant co-localization (Figure S3C). Interestingly, the overall TOBF1 protein levels did not change during the cell cycle (Figures S3D and S3E), suggesting that TOBF1 transiently accumulates in foci at early G1. Collectively, these data show that *Panct1* and TOBF1 colocalize specifically at the early G1 phase in discrete nuclear foci and that this effect is independent of the protein turnover in these cells.

Since *Panct1* FISH signals overlapped with TOBF1 foci, we next investigated if depletion of *Panct1* influences the formation of TOBF1 foci. Strikingly, *Panct1* RNAi abolished the formation of TOBF1 foci in early G1 (Figure 3B), although no notable changes to total TOBF1 protein levels occurred (Figure S3F). To determine if *Panct1* and TOBF1 physically interact, we performed RNA immunoprecipitation (RIP) experiments. We indeed detected an enrichment of *Panct1* RNA after pulling down TOBF1 in comparison to a control lncRNA (Figure 3C), indicating that TOBF1 and *Panct1* interact either directly or through other factors. Interestingly, the signals were greater in G1-phase-enriched samples, indicating that the association of TOBF1 with *Panct1* is strongest in this phase of the cell cycle (Figure 3C).

## TOBF1 Shows Enrichment at Genomic Sites Harboring OCT-SOX Motif in Presence of *Panct1*

To investigate the observed TOBF1 foci in more detail, we performed high-resolution time-lapse imaging. Interestingly, this analysis revealed Brownian-motion-like movement of the TOBF1 spots reminiscent of chromosomal movements seen at the onset of interphase (Gerlich and Ellenberg, 2003; Heun et al., 2001) (Figures 3D, 3E, and S3G; Movie S2). Furthermore, correlative light and electron microscopy (CLEM) revealed bright fluorescent spots in DNA-dense regions, implying that TOBF1 might interact with DNA (Figure 3F).

To investigate whether TOBF1 binds to genomic DNA, we performed chromatin immunoprecipitation sequencing (ChIP-seq). Indeed, we identified more than 12,000 TOBF1 chromosomal binding regions (GEO: GSE73806), with the majority of the binding sites situated in the promoter regions of genes (Figure 3G; Table S1).

Closer inspection of TOBF1 binding sites revealed that a substantial number of peaks overlapped with reported POU5F1 binding sites (Whyte et al., 2013), but exhibited lower signal strength (Figure 3H). Since bright TOBF1 foci formation was observed during early G1, we performed ChIP-qPCR at different stages of the cell cycle and observed that the DNA occupancy of TOBF1 peaked at a time point when cells were in G1 phase, suggesting the possibility that the bright spots represented regions in the DNA that TOBF1 interacts with (Figures 4A and S3H). Surprisingly, the consensus sequence for TOBF1 binding sites obtained by *de novo* motif search analysis using Meme-ChIP (Machanick and Bailey, 2011) revealed the canonical OCT4-SOX2 (Oct-Sox) binding motif (Figure 4B), indicating that TOBF1 is an Oct-Sox motif binding protein. We observed that more than 79% of TOBF1 sites that contained the Oct-Sox motif overlapped with reported POU5F1 binding sites that also contain the same motif (Figure 4C), suggesting that these sites could be bound by both POU5F1 and TOBF1.

Several lncRNAs have been shown to mediate protein binding to specific DNA regions (Wang and Chang, 2011; Guttman and Rinn, 2012; Rinn and Chang, 2012). Based on the colocalization of *Panct1* and TOBF1, the disappearance of TOBF1 foci after *Panct1* RNAi and the physical association of *Panct1* and TOBF1 in early G1 phase, we hypothesized that *Panct1* might facilitate the recruitment of TOBF1 to Oct-Sox sequences. Consistent with this idea, *Panct1* KO cells showed a strong reduction in binding of TOBF1 to promoters of pluripotency genes (Figure S3I). Curiously, we also observed that POU5F1 occupancy at important pluripotency regulatory regions was reduced in the *Panct1* KO cells, indicating that deletion of *Panct1* also compromises the binding of POU5F1 to its target sites (Figure 4D). We conclude that *Panct1* is required for efficient recruitment of TOBF1 and POU5F1 to their target sites on DNA.

## An OCT-SOX Motif in the *Panct1* Sequence Is Important for Its Function

We finally turned our attention to dissecting how *Panct1* might facilitate TOBF1 binding to its target sites in the genome. To inquire if this process might involve *Panct1* interaction with DNA, we used chromatin isolation by RNA purification (ChIRP) to address potential *Panct1* binding sites across the genome

(D) Quantification of (C). Error bars indicate the SEM from three biological replicates.
(E) Western blot showing depletion of TOBF1-GFP (BAC tagged) 96 hr after transfection with *Tobf1* esiRNA compared to control transfection (Luc). Protein molecular weights are indicated on the right.
(F) Western blot showing TOBF1 levels at the indicated time points after onset of differentiation.
(G) Representative immunofluorescence (IF) of TOBF1-GFP showing localization in mouse ESCs (cyan). Bottom panel shows cells with punctate foci visible in a subset of asynchronically growing cells. DNA is counterstained with DAPI and represented in red. Scale bars, 5 μm.
(H) Representative image of combined RNA FISH (red) and IF (green) showing co-localization of *Panct1* and TOBF1 in cells with TOBF1 foci. Arrows mark colocalized spots. DNA is counterstained with DAPI and represented in blue. Scale bar 5, μm.
(I) Boxplot showing the percentage of overlap between TOBF1 IF spots with *Panct1* FISH signals and *Panct1* FISH signals with TOBF1 IF spots, respectively (n = 14 cells). Whiskers show distribution of overlap. Actual values are represented by dark triangles. **p < 0.01; ***p < 0.005 (two-tailed Student's t test).

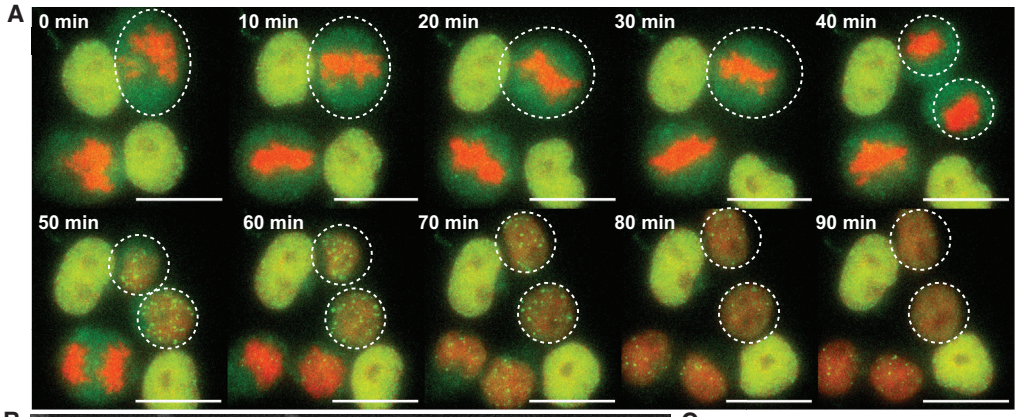


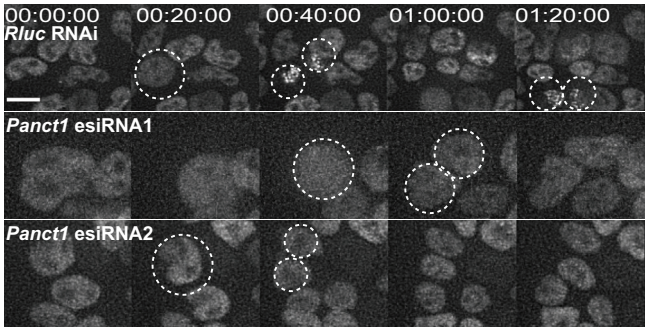


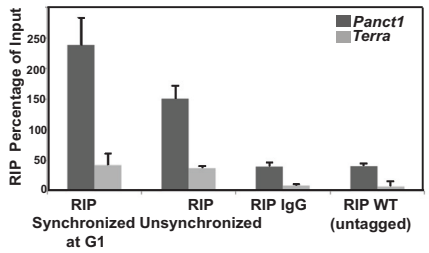


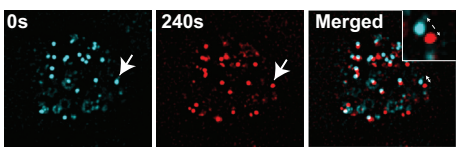


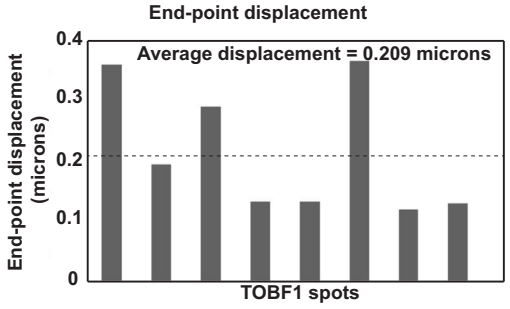


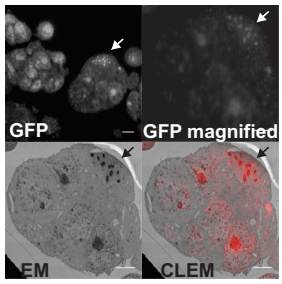


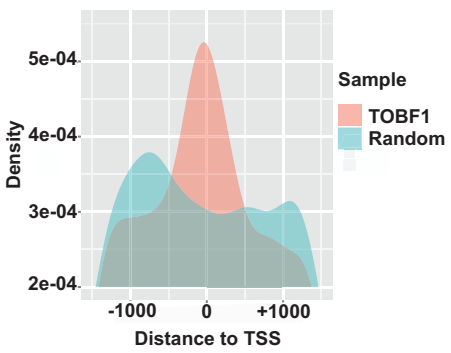


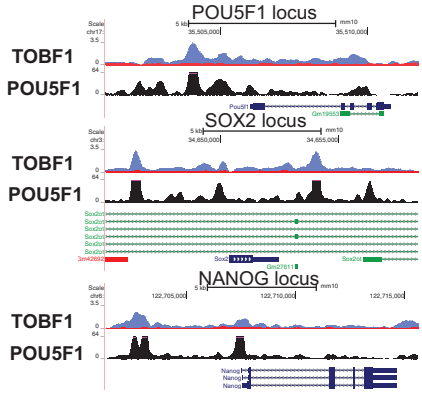


*(legend on next page)*

using two sets of biotinylated probes spanning *Panct1* (Chu et al., 2011; Quinn et al., 2014) and further refined the quality of the data by performing the same assay in the *Panct1* KO cell line (GEO: GSE73806; Figure S4A). To elucidate if there was any correlation between the *Panct1* and TOBF1 binding sites, we then focused on loci where they overlapped and identified 285 binding sites across the genome where a TOBF1 peak, a *Panct1* peak, and an Oct-Sox motif overlapped (Figure S4B; Table S2). Interestingly, TOBF1 ChIP enrichment at these sites was higher than at non-*Panct1* binding sites ($p = 1.59 \times 10^{-12}$, Wilcoxon rank-sum test), indicating that binding of the protein is particularly strong at sites of strong *Panct1* binding. Collectively, these data reveal that *Panct1* potentially interacts with genomic DNA and shows significant co-occupancy with TOBF1 on Oct-Sox motifs in mouse ESCs.

lncRNAs are known to interact with DNA either by direct base pairing or through protein intermediates (Rinn, 2014; Zhang et al., 2014). Markedly, the *Panct1* transcript itself contains a sequence stretch complementary to the Oct-Sox motif (Figure 4E). We speculated that this sequence stretch might mediate the lncRNA-DNA interaction, which in turn facilitates TOBF1 recruitment at sites containing the Oct-Sox motif. To test this, we scrambled the sequence of this motif and tested the mutant version of *Panct*1 (Figure 4F) in a panel of assays. Overexpression of *Panct1* in the KO background rescued the reduced AP staining seen in these cells. In contrast, overexpression of mutant *Panct1* was unable to rescue the phenotype, suggesting that the Oct-Sox motif within the *Panct1* transcript is important for its function (Figures S4C and S4D). Consistent with this observation, overexpression of mutant *Panct1* in wild-type (WT) ESCs caused a reduction in the intensity of TOBF1 spots seen in early G1 phase of the cell cycle (Figure S4E). To investigate if this reduced TOBF1 intensity might reflect reduced genomic recruitment of the protein in such cells due to the inability of *Panct1* to bind to TOBF1, we performed TOBF1 ChIP at pluripotency loci and observed a decrease in TOBF1 occupancy upon overexpression of mutant *Panct1* (Figure S4F).

Since *Panct1* KO cells had shown reduced POU5F1 binding to DNA (Figure 4D), we finally investigated if mutant *Panct1* might also impact POU5F1 expression or its recruitment to chromatin. Strikingly, both POU5F1 expression and its recruitment to chromatin were indeed compromised upon mutant *Panct1* overexpression, suggesting that the Oct-Sox motif in *Panct1* is an important component of lncRNA's role in pluripotency maintenance (Figures 4G, S4G, and S4H). Taken together, these findings suggest that the mutated Oct-Sox motif in *Panct1* behaves as a dominant-negative mutation to affect wild-type *Panct1* function.

## DISCUSSION

In this study, we present the functional characterization of *Panct1*, a nuclear lncRNA expressed in mouse ESCs and important for pluripotency maintenance. We show that *Panct1* plays a role in coordinating the genomic recruitment of a putative DNA-interacting protein, TOBF1, in a cell-cycle-specific manner (Figure 4H). The exceptional cross-talk between *Panct1* and TOBF1 and their precise cellular interaction in nuclear foci in early G1, together with their regulation of pluripotency genes, provide a model of lncRNA activity that has multiple layers of coordinated control. Given that numerous intronic lncRNAs like *Panct1* are known to exist in nature, our study reveals that such a mode of action might represent a distinct subset of intronic lncRNA function.

The recruitment of TOBF1 to chromatin in the early G1 equates with the crucial point in normal cell-cycle progression when the first DNA binding factors are reassembled (Osborne et al., 2004; Yan et al., 2013). The role played by *Panct1* in establishing protein-DNA contacts might reflect a more general mechanism of lncRNA action in identifying genomic binding sites for factors that have been evicted during mitosis. lncRNAs might act as licensing factors for such events or provide scaffolds where proteins can assemble in a specific cellular context.

A curious observation of *Panct1* function is seen while overexpressing the mutant version of lncRNA where the Oct-Sox motif has been scrambled. Mutant *Panct1* inhibits endogenous *Panct1* activity by potentially sequestering TOBF1, thereby reducing TOBF1 occupancy on chromatin and decreasing intensity of early G1 foci. Further studies are required to understand how *Panct1* identifies and binds DNA and whether the Oct-Sox motif in *Panct1* makes physical contacts with DNA through canonical

**Figure 3. TOBF1 Localizes to DNA in a Cell-Cycle-Specific Manner**

(A) Time-lapse montage of TOBF1-GFP ESCs transfected with histone-2B-mCherry (red) showing TOBF1 localization (green) during the cell cycle. Dotted circles demarcate cells with the appearance of bright foci. Scale bars, 5 μm.

(B) Depletion of *Panct1* affects formation of TOBF1 spots in early G1 phase. Representative time-lapse images show a reduction in TOBF1 spots upon *Panct1* RNAi using 2 different esiRNAs. Renilla Luciferase (RLuc) RNAi serves as a control. Dotted circles demarcate daughter cells after mitosis. Note the absence of TOBF1 foci in *Panct1*-depleted cells at comparable overall TOBF1 levels.

(C) TOBF1 and *Panct1* interact in early G1 phase. RIP of TOBF1 enrichment is shown for indicated lncRNAs. Error bars indicate the SEM of three PCR replicates. Data are representative of 2 experiments.

(D) TOBF1 shows a dynamic localization pattern in early G1 phase. Representative images of a cell show foci and the endpoint displacement of the same foci (denoted by arrow) after a time period of 4 min. White bidirectional arrow represents a displacement of 0.516 μm calculated from pixel units.

(E) Endpoint displacement of 8 TOBF1 foci over time (in microns). Dotted line represents average endpoint displacement.

(F) CLEM showing localization of TOBF1 foci. Grayscale images showing light microscopy of GFP (top panel) and EM images of same cells showing colocalization with nuclear structures (bottom panel). Arrow marks a region from which the EM signal has been acquired. Scale bar in top-left image represents 10 μm and 4 μm for all subsequent images.

(G) Distribution of TOBF1 peaks close to transcription start sites as compared to an analogous distribution of random set of genomic sites. x axis represents distance of peak to transcription start site (TSS) in base pairs, and y axis represents probability density of the peaks.

(H) TOBF1 binding sites overlap with reported POU5F1 binding sites. Representative images of UCSC gene tracks depict the TOBF1 peaks (blue) and POU5F1 (Whyte et al., 2013) binding sites (black). Input track is overlaid in red.

See also Figure S3.

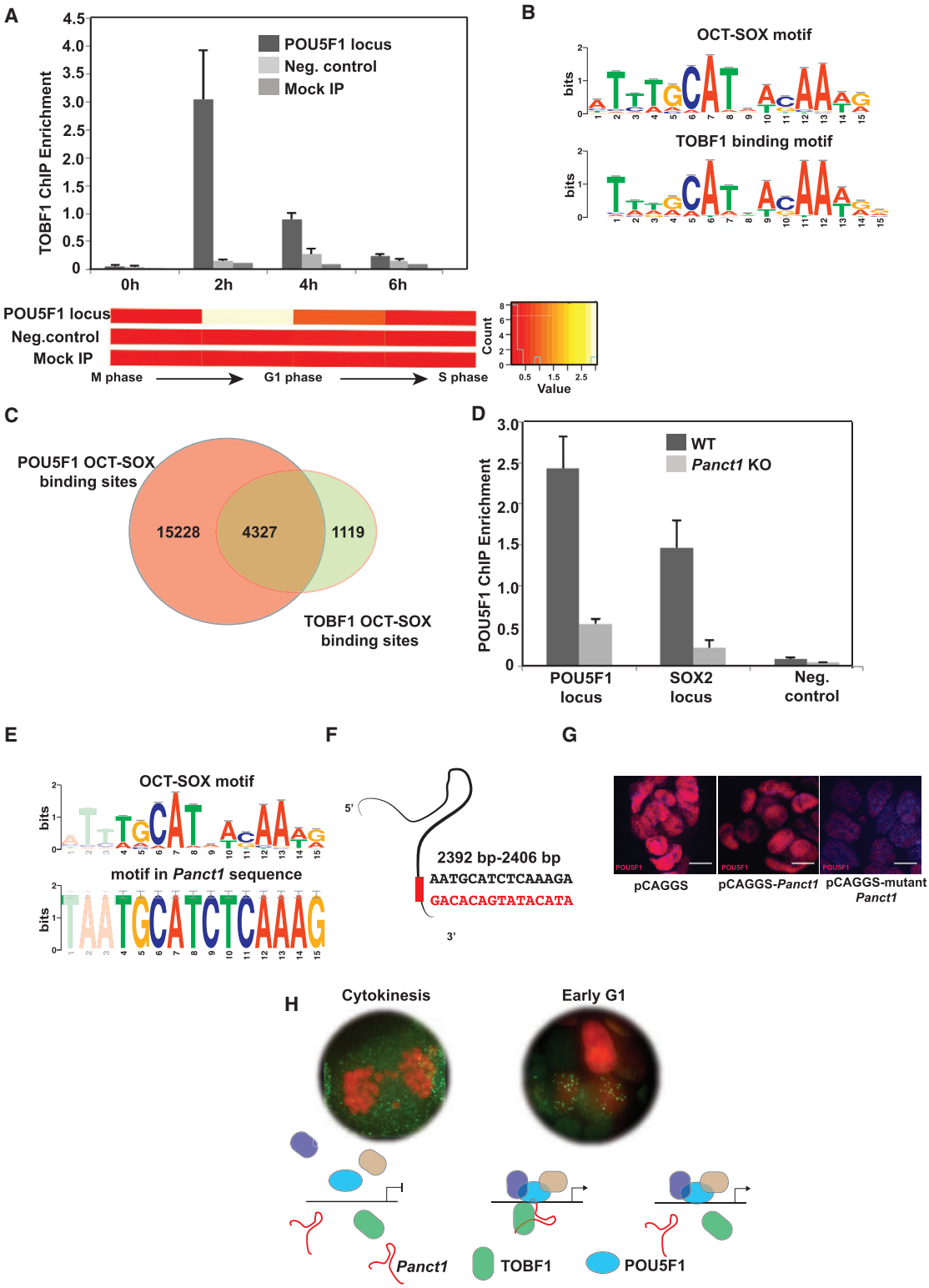


**Figure 4. Panct1 Recruits TOBF1 via an OCT-SOX Motif**

(A) TOBF1 is enriched at loci of pluripotency genes during G1. Chromatin immunoprecipitation (ChIP) enrichment at the POU5F1 distal enhancer at the indicated time points following release from M phase arrest is represented as the percentage of input and denoted on the y axis. ChIP at a non-specific locus and mock IP are shown as negative controls. Error bars indicate the SEM of three PCR replicates. Data are representative of 3 experiments.

*(legend continued on next page)*

lncRNA:DNA interactions such as base pairing or triple helix formation.

The competition with a mutated lncRNA could present an interesting opportunity for regulating the behavior of DNA-binding proteins and could potentially be utilized for manipulating the dynamics of such proteins. Altering the motif to recognize other sites in the genome might offer the possibility to drive cellular cargo to specific addresses through an lncRNA-mediated delivery system.

## EXPERIMENTAL PROCEDURES

### Cell Culture and Transfection

ESCs (E14TG2a, R1/E) were cultured in DMEM supplemented with 4.5 g/L D-glucose and pyruvate (Invitrogen, 41966-029), 10% fetal bovine serum (Pan Biotech, P29-0705-ES), 30 μM β-mercaptoethanol (Invitrogen, 31350-010), 0.6X NEAA (Life Technologies, 11140-035), 300 units of penicillin/streptomycin (Invitrogen, 15070-063), and 8 ng/ml LIF (MPI-CBG, Dresden, Germany) per 500 mL of media. Media were changed every day, and ESCs were detached by treatment with trypsin-EDTA (PAA, L11-004) and split every 2 days. Cells were incubated at 37°C and 5% $CO_2$.

### Generating *Panct1* KO ESCs

For generating the *Panct1* targeting construct, a genomic sequence that contains 4-kb 5′ homology and 4.8-kb 3′ homology was subcloned from a BAC (RP24-87C20) into a p15A vector using recombineering technology. A LacZ-neo-pA cassette flanked by FRT sites was inserted upstream of the *Panct1* lncRNA that was flanked by loxP sites. The targeting construct was electroporated in R1 ESCs (129 genetic background) using standard protocols, and resistant colonies were selected using 0.2 mg/mL G418. Correct targeting events were identified by Southern hybridization using a 5′- and a 3′-external probe. The selection cassette was excised by Flpo-mediated recombination in ESCs, and, subsequently, the Cre-ERT2 recombinase was targeted to the Rosa26 locus. For details of genotyping primers and deleting *Panct1* in TOBF1 BAC, see the Supplemental Experimental Procedures.

### Quantification and Statistical Analysis

Sample size determination followed standard practices and experiments reported in literature; no estimates were performed to ensure adequate power to a pre-specified effect size. No blinding or randomization was done during sample allocation. Statistical analysis was performed using standard statistical tools available in Microsoft Excel or as reported in the Supplemental Experimental Procedures. Statistical details including statistical tests used and the type and values of replicates for every experiment can be found in the accompanying figure legends.

### RNA FISH

RNA FISH was performed as described previously (Chakraborty et al., 2012), with fluorescently labeled riboprobes. For details, see the Supplemental Experimental Procedures.

### ChIRP

The ChIRP experiment was performed using biotin-TEG-labeled probes as described previously (Chu et al., 2011). For details, see the Supplemental Experimental Procedures.

Further details and an outline of resources used in this work can be found in Supplemental Experimental Procedures.

## DATA AND SOFTWARE AVAILABILITY

The accession number for all data from TOBF1 ChIP and ChIRP sequencing reported in this paper is GEO: GSE73806.

## SUPPLEMENTAL INFORMATION

Supplemental Information includes Supplemental Experimental Procedures, four figures, two tables, and two movies and can be found with this article online at https://doi.org/10.1016/j.celrep.2017.11.045.

## ACKNOWLEDGMENTS

We thank the Light Microscopy Facility (MPI-CBG, Dresden) and the Electron Microscopy Facility (MPI-CBG, Dresden), especially Kimberly Gibson and Jean Marc Verbavatz for help with microscopy. We are thankful to the Deep Sequencing Facility (CRTD) for performing next-generation sequencing. We are grateful to the BAC transgenomics facility (MPI-CBG) for generating the BAC-tagged cell lines used in this study. We are thankful to Mandy Obst and Doris Mueller for generating the conditional *Panct1* knockout ESCs; Eupheria Biotec and especially Sebastian Rose and Romy Zschau for providing esiRNAs used in this study; and the entire Buchholz lab for helping generously with experiments and intellectual input. This work was supported by a grant from the Bundesministerium für Bildung und Forschung (0315980), an EU FP7 grant SyBoSS (242129), and grants from the Deutsche Forschungsgemeinschaft (SPP1356, BU1400/5-1, and SFB655) (B5).

## AUTHOR CONTRIBUTIONS

Conceptualization, D.C., J.M., A.F.S., K.A., C.C., and F.B.; Investigation, D.C., N.B., L.D., V.I., and J.F.; Analysis, M.P.-R. and D.C.; Writing, D.C. and F.B.

## DECLARATION OF INTERESTS

The authors declare no competing interests.

Received: May 24, 2017
Revised: October 13, 2017
Accepted: November 13, 2017
Published: December 12, 2017

## REFERENCES

Aksoy, I., Giudice, V., Delahaye, E., Wianny, F., Aubry, M., Mure, M., Chen, J., Jauch, R., Bogu, G.K., Nolden, T., et al. (2014). Klf4 and Klf5 differentially inhibit

(B) Consensus motif analysis of TOBF1 peaks. Vertical axis represents bit score featuring the prevalence of an individual nucleotide at a given position. Horizontal axis represents base position and the likelihood of finding a given nucleotide at that position. The POU5F1 consensus-binding motif is presented as a comparison.
(C) Venn diagram shows the overlap of TOBF1 and POU5F1 peaks containing the OCT-SOX motif.
(D) POU5F1 binding to pluripotency gene promoters is affected upon *Panct1* depletion. ChIP showing POU5F1 occupancy at *Pou5f1* and *Sox2* locus in WT and *Panct1* KO cells depicted as fold enrichment over mock. A non-specific genomic locus is presented as a negative control. Error bars indicate the SEM of three PCR replicates. Data are representative of 2 experiments.
(E) Alignment of the OCT-SOX consensus-binding motif with a sequence present in *Panct1* (faded region shows non-matching sequences).
(F) Sequence of the scrambled Octamer motif aligned to the *Panct1* sequence. The original sequence is marked in black, and the mutated sequence is denoted in red.
(G) Representative POU5F1 immunofluorescence in WT ESCs transfected with overexpression constructs as indicated. Note the reduction of POU5F1 expression in cells transfected with mutant *Panct1*.
(H) Schematic model for *Panct1* function in mouse ESCs. Colored boxes represent *Panct1*, TOBF1, or POU5F1 as indicated.
See also Figure S4.

mesoderm and endoderm differentiation in embryonic stem cells. Nat. Commun. *5*, 3719.

Chakraborty, D., Kappei, D., Theis, M., Nitzsche, A., Ding, L., Paszkowski-Rogacz, M., Surendranath, V., Berger, N., Schulz, H., Saar, K., et al. (2012). Combined RNAi and localization for functionally dissecting long noncoding RNAs. Nat. Methods *9*, 360–362.

Chu, C., Qu, K., Zhong, F.L., Artandi, S.E., and Chang, H.Y. (2011). Genomic maps of long noncoding RNA occupancy reveal principles of RNA-chromatin interactions. Mol. Cell *44*, 667–678.

Dinger, M.E., Amaral, P.P., Mercer, T.R., Pang, K.C., Bruce, S.J., Gardiner, B.B., Askarian-Amiri, M.E., Ru, K., Soldà, G., Simons, C., et al. (2008). Long noncoding RNAs in mouse embryonic stem cell pluripotency and differentiation. Genome Res. *18*, 1433–1445.

Engreitz, J.M., Ollikainen, N., and Guttman, M. (2016). Long non-coding RNAs: spatial amplifiers that control nuclear structure and gene expression. Nat. Rev. Mol. Cell Biol. *17*, 756–770.

Gerlich, D., and Ellenberg, J. (2003). Dynamics of chromosome positioning during the cell cycle. Curr. Opin. Cell Biol. *15*, 664–671.

Guil, S., Soler, M., Portela, A., Carrère, J., Fonalleras, E., Gómez, A., Villanueva, A., and Esteller, M. (2012). Intronic RNAs mediate EZH2 regulation of epigenetic targets. Nat. Struct. Mol. Biol. *19*, 664–670.

Guttman, M., and Rinn, J.L. (2012). Modular regulatory principles of large non-coding RNAs. Nature *482*, 339–346.

Guttman, M., Donaghey, J., Carey, B.W., Garber, M., Grenier, J.K., Munson, G., Young, G., Lucas, A.B., Ach, R., Bruhn, L., et al. (2011). lincRNAs act in the circuitry controlling pluripotency and differentiation. Nature *477*, 295–300.

Hacisuleyman, E., Goff, L.A., Trapnell, C., Williams, A., Henao-Mejia, J., Sun, L., McClanahan, P., Hendrickson, D.G., Sauvageau, M., Kelley, D.R., et al. (2014). Topological organization of multichromosomal regions by the long intergenic noncoding RNA Firre. Nat. Struct. Mol. Biol. *21*, 198–206.

Heo, J.B., and Sung, S. (2011). Vernalization-mediated epigenetic silencing by a long intronic noncoding RNA. Science *331*, 76–79.

Heun, P., Laroche, T., Shimada, K., Furrer, P., and Gasser, S.M. (2001). Chromosome dynamics in the yeast interphase nucleus. Science *294*, 2181–2186.

Hutchins, J.R., Toyoda, Y., Hegemann, B., Poser, I., Hériché, J.K., Sykora, M.M., Augsburg, M., Hudecz, O., Buschhorn, B.A., Bulkescher, J., et al. (2010). Systematic analysis of human protein complexes identifies chromosome segregation proteins. Science *328*, 593–599.

Kittler, R., Pelletier, L., Ma, C., Poser, I., Fischer, S., Hyman, A.A., and Buchholz, F. (2005). RNA interference rescue by bacterial artificial chromosome transgenesis in mammalian tissue culture cells. Proc. Natl. Acad. Sci. USA *102*, 2396–2401.

Li, Z., Huang, C., Bao, C., Chen, L., Lin, M., Wang, X., Zhong, G., Yu, B., Hu, W., Dai, L., et al. (2015). Exon-intron circular RNAs regulate transcription in the nucleus. Nat. Struct. Mol. Biol. *22*, 256–264.

Lin, N., Chang, K.-Y., Li, Z., Gates, K., Rana, Z.A., Dang, J., Zhang, D., Han, T., Yang, C.S., Cunningham, T.J., et al. (2014). An evolutionarily conserved long noncoding RNA *TUNA* controls pluripotency and neural lineage commitment. Mol. Cell *53*, 1005–1019.

Loewer, S., Cabili, M.N., Guttman, M., Loh, Y.H., Thomas, K., Park, I.H., Garber, M., Curran, M., Onder, T., Agarwal, S., et al. (2010). Large intergenic non-coding RNA-RoR modulates reprogramming of human induced pluripotent stem cells. Nat. Genet. *42*, 1113–1117.

Machanick, P., and Bailey, T.L. (2011). MEME-ChIP: motif analysis of large DNA datasets. Bioinformatics *27*, 1696–1697.

Martello, G., and Smith, A. (2014). The nature of embryonic stem cells. Annu. Rev. Cell Dev. Biol. *30*, 647–675.

McHugh, C.A., Chen, C.K., Chow, A., Surka, C.F., Tran, C., McDonel, P., Pandya-Jones, A., Blanco, M., Burghard, C., Moradian, A., et al. (2015). The Xist lncRNA interacts directly with SHARP to silence transcription through HDAC3. Nature *521*, 232–236.

Osborne, C.S., Chakalova, L., Brown, K.E., Carter, D., Horton, A., Debrand, E., Goyenechea, B., Mitchell, J.A., Lopes, S., Reik, W., and Fraser, P. (2004). Active genes dynamically colocalize to shared sites of ongoing transcription. Nat. Genet. *36*, 1065–1071.

Poser, I., Sarov, M., Hutchins, J.R., Hériché, J.K., Toyoda, Y., Pozniakovsky, A., Weigl, D., Nitzsche, A., Hegemann, B., Bird, A.W., et al. (2008). BAC TransgeneOmics: a high-throughput method for exploration of protein function in mammals. Nat. Methods *5*, 409–415.

Quinn, J.J., Ilik, I.A., Qu, K., Georgiev, P., Chu, C., Akhtar, A., and Chang, H.Y. (2014). Revealing long noncoding RNA architecture and functions using domain-specific chromatin isolation by RNA purification. Nat. Biotechnol. *32*, 933–940.

Rinn, J.L. (2014). lncRNAs: linking RNA to chromatin. Cold Spring Harb. Perspect. Biol. *6*, 6.

Rinn, J.L., and Chang, H.Y. (2012). Genome regulation by long noncoding RNAs. Annu. Rev. Biochem *81*, 145–166.

Sheik Mohamed, J., Gaughwin, P.M., Lim, B., Robson, P., and Lipovich, L. (2010). Conserved long noncoding RNAs transcriptionally regulated by Oct4 and Nanog modulate pluripotency in mouse embryonic stem cells. RNA *16*, 324–337.

Tsai, M.C., Manor, O., Wan, Y., Mosammaparast, N., Wang, J.K., Lan, F., Shi, Y., Segal, E., and Chang, H.Y. (2010). Long noncoding RNA as modular scaffold of histone modification complexes. Science *329*, 689–693.

Ulitsky, I., and Bartel, D.P. (2013). lincRNAs: genomics, evolution, and mechanisms. Cell *154*, 26–46.

Wang, K.C., and Chang, H.Y. (2011). Molecular mechanisms of long noncoding RNAs. Mol. Cell *43*, 904–914.

Whyte, W.A., Orlando, D.A., Hnisz, D., Abraham, B.J., Lin, C.Y., Kagey, M.H., Rahl, P.B., Lee, T.I., and Young, R.A. (2013). Master transcription factors and mediator establish super-enhancers at key cell identity genes. Cell *153*, 307–319.

Yan, J., Enge, M., Whitington, T., Dave, K., Liu, J., Sur, I., Schmierer, B., Jolma, A., Kivioja, T., Taipale, M., and Taipale, J. (2013). Transcription factor binding in human cells occurs in dense clusters formed around cohesin anchor sites. Cell *154*, 801–813.

Young, R.A. (2011). Control of the embryonic stem cell state. Cell *144*, 940–954.

Zhang, H., Zeitz, M.J., Wang, H., Niu, B., Ge, S., Li, W., Cui, J., Wang, G., Qian, G., Higgins, M.J., et al. (2014). Long noncoding RNA-mediated intrachromosomal interactions promote imprinting at the *Kcnq1* locus. J. Cell Biol. *204*, 61–75.